Journal of Physics: Conference Series

Merged beam studies of mutual neutralization at subthermal collision energies

Merged beam studies of mutual neutralization at subthermal collision energies

X. Urbain[1], N. de Ruette[2,3], A. Dochain[1], T. Launoy[4], R.F. Nascimento[2], M. Kaminska[2], M.H. Stockett[2], J. Loreau[4], J. Liévin[4], N. Vaeck[4], R.D. Thomas[2], H.T. Schmidt[2] and H. Cederquist[2]

[1] Institute of Condensed Matter and Nanosciences, Université catholique de Louvain, B-1348 Louvain-la-Neuve, Belgium
[2] Department of Physics, Stockholm University, Stockholm, SE-106 91, Sweden
[3] European Spallation Source ESS AB, P.O. Box 176, SE-211 00 Lund, Sweden
[4] Laboratoire de Chimie Quantique et Photophysique, Université Libre de Bruxelles, B-1050 Brussels, Belgium

E-mail: xavier.urbain@uclouvain.be

Abstract. We have measured the kinetic energy distributions for the mutual neutralization of a large ensemble of atomic anions and cations. Ions are accelerated to equal velocities in a merged beam setup, enabling measurements at collision energies as low as 5 meV. Three-dimensional momentum imaging is performed with two position sensitive detectors located several meters downstream from the few centimeter long region where the beams overlap. An unprecedented resolution in the kinetic energy release (KER) spectra allows us to identify the states of both reactants and products down to their fine structure. Knowing the angular distribution of the products in the laboratory and center-of-mass frame, allows for total, partial, and differential cross sections to be retrieved.

1. Introduction

Anions are present in a variety of astrophysical environments [1]. Their presence in molecular clouds has been confirmed quite recently with the detection of C_6H^- [2], soon to be followed by C_4H^- [3], C_8H^- [4], C_3N^- [5], C_5N^- [6], and lately CN^- [7]. They are thought to be the main reservoir of negative charges in cold and dense environments. While radiative and dissociative attachment are thought to be their dominant formation route, mutual neutralization would constitute an important destruction mechanism besides photodetachment [8].

Vuitton *et al* [9] characterized the abundance and role of CN^- and C_3N^- anions in the chemistry of Titan's upper atmosphere. More importantly, they identified associative detachment to radical species as the major destruction pathway. Closer to us, the role of oxygen anions in Earth's upper atmosphere is clearly established [10]. Electrons attach to oxygen on the night side, and ionospheric reactions take place that produce characteristic nightglows. Satellite images of the UV tropical nightglow of O I at 135.6 nm have been interpreted as resulting for a large part from the mutual neutralization reaction $O^- + O^+ \rightarrow O(^5P) + O$, followed by the radiative cascade $O(^5P) \rightarrow O(^5S) \rightarrow O(^3P)$ (note that the first emission at 777 nm is also observed) [11, 12]. Finally, high-resolution spectroscopy of trace metallic elements present in the outer layers of stellar objects is now widely available [13]. A quantitative interpretation

of those spectra in terms of elemental abundances can only be reached through non-local thermodynamic equilibrium (non-LTE) stellar atmosphere modeling [14], which in turn requires full understanding of the ion-pair to covalent transitions responsible for collisional excitation between neutrals and mutual neutralization between ions [15, 16].

Of more practical application is the role played by negative ions in technical plasmas, the most obvious being the large scale production of high energy, high current negative deuterium beams as precursors of powerful neutral beams [17]. Their tangential injection into the toroidal plasma of tokamaks like ITER should increase the plasma temperature beyond the point where ohmic heating becomes inefficient. Volume production of D^- is normally impeded by the concurrent neutralization with D^+, D_2^+ and D_3^+ cations [18]. This limitation has been overcome by means of cesiated surfaces increasing the relative abundance of low energy electrons and the partitioning of the plasma volume between hot ionization and colder recombination regions, with the help of magnetic grids [19].

2. Mutual neutralization

Subthermal collisions, *i.e.*, collisions at velocities typical of a cold gas, do not necessarily proceed along weakly attractive potentials nor do they exhibit long-range potential barriers limiting the rate coefficient to some finite value. Indeed, anion-cation collisions are dominated by the long-range Coulomb attraction that captures increasingly large impact parameters as the collision velocity is reduced. Such processes have diverging rate coefficients as allowed by Wigner's threshold law. The reaction channels that are accessible at low energy are:

$$\begin{aligned} A^+ + B^- &\rightarrow A^* + B^* && \text{MN} && (1)\\ &\rightarrow A + B^+ + e^- && \text{TI} && (2)\\ &\rightarrow A^- + B^+ && \text{CX} && (3)\\ &\rightarrow AB^+ + e^- && \text{AI} && (4) \end{aligned}$$

where MN stands for mutual neutralization, TI for transfer ionization, CX for (double) charge exchange and AI for associative ionization (see [20] for a review). When dealing with polyatomic systems, e.g. $H_2^+ + O^-$ [21] and $CH^+ + O^-$ [22], one may further distinguish:

$$\begin{aligned} AB^+ + C^- &\rightarrow AC^* + B && \text{RN} && (5)\\ &\rightarrow AC^+ + B + e^- && \text{RI} && (6)\\ &\rightarrow ABC + h\nu && \text{RA} && (7) \end{aligned}$$

where RN stands for reactive neutralization, RI for reactive ionization, and RA for radiative association. For the latter process to occur, a long-lived resonance must be formed, for the radiative stabilization to compete with the predissociation of the collisional complex.

Due to energy conservation, the energy imparted to mutual neutralization products reflects their degree of internal excitation. This exoergicity will be referred to as the (total) kinetic energy release (KER):

$$\begin{aligned} A^+ + B^- &\rightarrow A^* + B^* + \text{KER} && (8)\\ \text{KER} &= [IP(A) - E_{exc}(A^*)] - [EA(B) + E_{exc}(B^*)] && (9) \end{aligned}$$

where IP is the ionization potential of atom A, E_{exc} its excitation energy, and EA the electron affinity of atom B. A schematic potential energy diagram is given in Figure 1 for the $O^+ + O^-$ reaction. As discussed below, the electron transfer will preferably occur at the crossing points

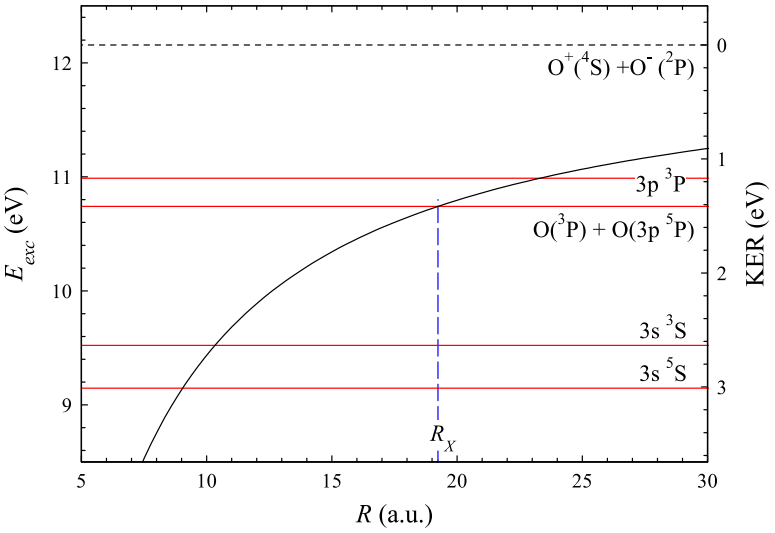

Figure 1. Diabatic potential energy diagram (schematic) for the $O^+ + O^-$ mutual neutralization. The excitation energy E_{exc} of $O(2s^2 2p^3 nl\, ^{2S+1}L)$ levels is converted to the kinetic energy release KER by means of Eq. 9. R_X is the internuclear distance at which electron transfer takes place.

constant potentials corresponding to the various covalent channels situated *below* the incoming asymptote. The experimental challenge will therefore be to energetically resolve these outgoing channels while collecting all mutual neutralization products, thereby obtaining total and partial MN cross sections. These will eventually benchmark theoretical calculations giving complete access to the full scattering matrix, *i.e.*, excitation, deexcitation, mutual neutralization and ion pair formation reactions. We describe hereafter some recent advances towards the completion of this task.

3. Single-pass merged beam experiment

In order to manipulate ion beams of different species and bring them to low relative collision velocities, we opt for the well-established merged beam arrangement (see [23] for a review). In this configuration, collimated beams of fast ions are brought into confluence at equal velocities, reducing the center-of-mass collision energy E_r to virtually zero. More precisely:

$$E_r = \mu \left[\frac{E_1}{M_1} + \frac{E_2}{M_2} - 2\sqrt{\frac{E_1 E_2}{M_1 M_2}} \cos\phi \right] \simeq \frac{\mu}{M_1} E_1 \phi^2 \tag{10}$$

where E_1, M_1, E_2 and M_2 stand for the laboratory energies and masses of colliding ions, with $E_1/M_1 \simeq E_2/M_2$, μ is the reduced mass and ϕ is the average angle formed by the interacting beams. As a consequence, beam energies have to be scaled according to the mass ratio between the species under study, which limits the range of applicability of the method. In the set-up depicted on Figure 2 [24, 25], cations and anions are first accelerated and brought along parallel trajectories, to be electrostatically merged by two pairs of parallel plates mounted on a movable assembly. This motion is required to fulfil the merging criterion, *i.e.*, they must enter the last steering element at an angle that is inversely proportional to their kinetic energy for them to come out parallel to one another. Detuning the collision energy from near-zero to a finite and controlled value is performed by applying some electrical bias to the interaction cell located in the UHV section of the apparatus ($\sim 10^{-10}$ mbar). Reaction products may be charged or neutral. For mutual neutralization studies, both ion beams are dumped at the exit of the UHV region, while the neutrals fly unaffected towards the detection system located 3 to 5 m downstream. For the simple case of particles of equal velocity v and laboratory energy E, the kinetic energy release (KER) is related to the spatial (Δx) and temporal (Δt) separation of the

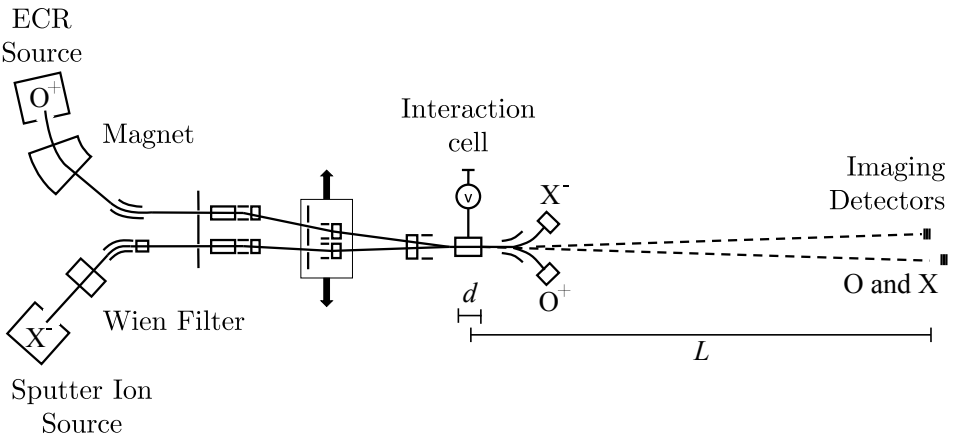

Figure 2. Schematics of the merged-beam apparatus for the study of $O^+ + X^-$ mutual neutralization. Ion sources are mounted on ±20 kV platforms. A duoplasmatron source was used for H^- and D^- anions.

products detected at a distance L from the interaction region:

$$\mathrm{KER} = \frac{E}{2L^2}\left[\Delta x^2 + v^2\Delta t^2\right] \tag{11}$$

The resolution of the KER measurement will strongly depend on the precision to which L is known, *i.e.*, on the ratio of the interaction length d to the average distance to the detectors. In the present case, $2 < d < 7.5$ cm and $L < 5$ m, producing a relative KER resolution of ~ 1 %.

Last, when dealing with merged electron and ion beams, it is common practice to describe their interaction in the co-moving frame by two temperatures, $T_{\|}$ and $T_{\perp}$. The former is a direct measure of the longitudinal velocity spread, while the latter reflects the collimation of the beams. The distribution of relative velocities reads:

$$f(v_d, \vec{v}) = \frac{m}{2\pi k T_{\perp}}\sqrt{\frac{m}{2\pi k T_{||}}}\exp\left[-\frac{m v_{\perp}^2}{2\pi k T_{\perp}} - \frac{m(v_{\|} - v_d)^2}{2\pi k T_{||}}\right] \tag{12}$$

where $v_{\|} \simeq |v|(1 \pm \Delta E/2E)$ and $v_{\perp} \simeq |v| \sin\phi$, and v_d is the so-called detuning velocity, *i.e.*, the average velocity difference imparted to the beams by their acceleration and/or the interaction cell bias. For 12 keV C^- and C^+ beams with 5 eV energy dispersion, and 1 mrad angular spread, $T_{\|} \simeq 8$ K and $T_{\perp} \simeq 70$ K, subthermal values indeed. Early attempts to measure MN cross sections were limited by the inherent difficulty of detecting pairs of particles hitting a single detector close in time and space. We circumvented this limitation by installing a pair of position sensitive detectors operating in coincidence. Their circular shape and the dead area between them requires some modeling to retrieve the actual momentum distribution.

4. Results and interpretation

A joint effort by UCLouvain and Stockholm University has allowed the measurement of MN reactions for a large number of systems: C^+, N^+ and O^+ in combination with D^-, C^-, O^-, Si^-, P^- and S^-. Figure 3 summarizes the findings in terms of kinetic energy release in the O^+ case, which directly correlate to the final electronic state of the oxygen atom. The anions are ordered according to the electron affinity, with tighter bound electrons in the anion occupying

MN with O^+ favors the $2s^2 2p^3\, 3p\, ^5P$ state with a branching fraction of 71 ± 9 % measured at 5 meV [25], in fair agreement with earlier theoretical predictions [10], *i.e.*, 42 % at 300 K. The ^3P state is however much less populated than originally estimated, *i.e.*, 15 ± 4 % against 46 %. Since the UV tropical nightglow of oxygen has two distinct components at 130.4 and 135.6 nm, corresponding to ^3S and ^5S respectively, a reevaluation of the actual role of MN may be in order.

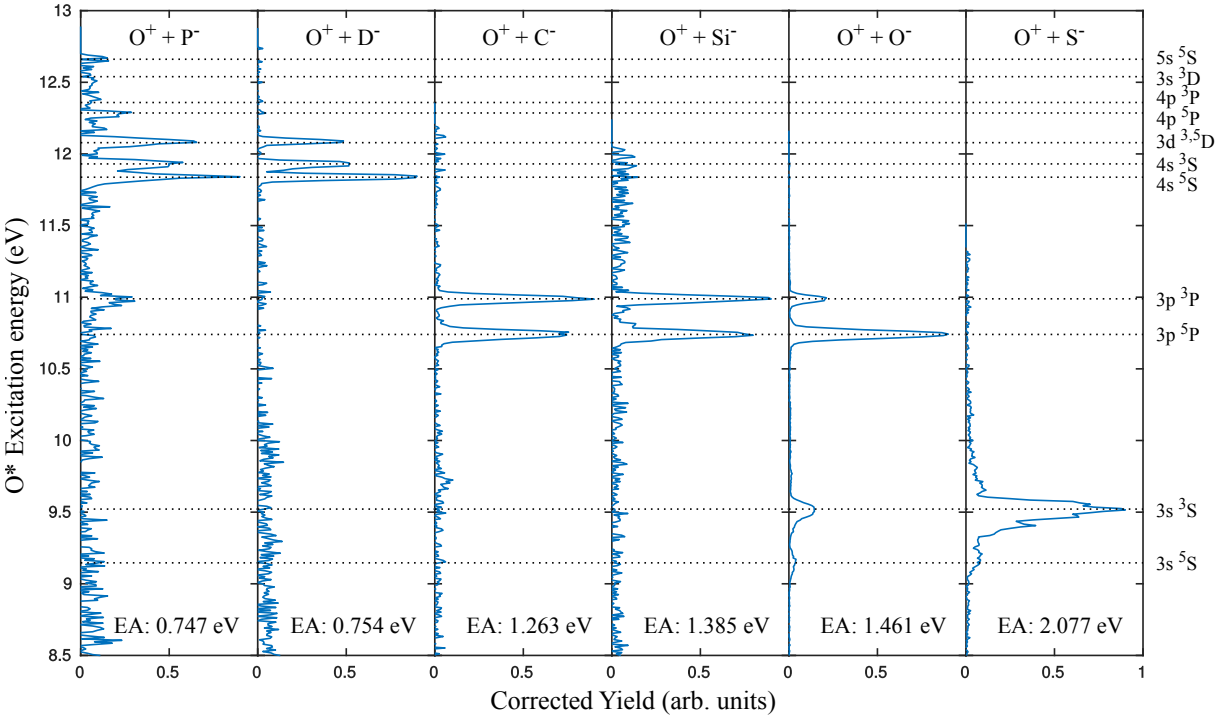

Figure 3. Kinetic energy release spectra for the $O^+ + X^-$ mutual neutralization. The energy scale is converted to the excitation energy of the $O(2s^2 2p^3 nl\, ^{2S+1}L)$ level by means of Eq. 9.

In order to rationalize the branching ratios measured for a wide variety of collisional systems, one is tempted to resort to a simplified treatment of the non-adiabatic interactions prevailing at the successive avoided crossings. A powerful approach is the Firsov-Landau-Herring asymptotic method [26] as applied by Zhou and Dickinson [27], that allows the evaluation of the one-electron exchange interaction $\Delta(R_X)$, where R_X is the crossing distance and $H_{if} \simeq \Delta(R_X)/2$ is approximately the coupling matrix element between states i and f, without explicitly treating the many-electron configuration interaction. These matrix elements are incorporated in a multi-state Landau-Zener calculation to generate total and partial cross sections. As shown by de Ruette *et al* [25], this single-electron treatment fails to reproduce the branching fractions observed in the case of $N^+ + O^-$, particularly for configurations like $N(2s2p^4\, ^4P)$ that involve two-electron processes. This discrepancy is partially lifted by introducing some configuration interaction among terms sharing the same symmetry, as obtained by multiconfiguration Hartree-Fock (MCHF) calculations. What remains is a systematic underestimation of the high-KER, *i.e.*, short R_X channels. As shown by Mitrushchenkov *et al* [28] for the $Ca^+ + H^-$ MN reaction, the two-by-two treatment applied in the multi-state LZ approach underestimates the contribution of weak transitions to the cross section that may be active at smaller internuclear distances. The more reliable branching probability current method [29] still lies beyond a current computational

to a full quantal treatment, as recently demonstrated by Launoy *et al* for the $Li^+ + H^-$ case [30]. Care must however be taken of the proper asymptotic description of the various channels, through the inclusion of diffuse orbitals.

5. Conclusions and perspectives

A single-pass merged beam apparatus has allowed us to collect a large ensemble of branching fractions among the various excited states produced by electron transfer in mutual neutralization reactions. We were able to assess the validity of earlier measurements and calculations, and to improve the theoretical treatment of such processes by including configuration interaction in the outgoing channels. Further experimental developments are needed to gain full access to the angular distribution of the products, which translates into state-specific differential cross sections. This total collection is needed to produce reliable cross sections. The forward detection is still impeded by the excessive background caused by rest-gas collisions. Such a limitation is absent in DESIREE, the double cryogenic storage ring facility located at Stockholm University [31, 32], where beams of anions and cations circulating in juxtaposed storage rings interact in a common straight section. Beams of anions and cations are stored for long times, allowing them to relax to their lowest quantum states [33]. This is particularly relevant for molecular species which can not be cooled in a continuous, single pass experiment. Such data are urgently needed for the astrochemical modeling of dense clouds and planetary atmospheres.

Acknowledgments

This work was supported by the Fonds de la Recherche Scientifique–FNRS (IISN Contract No. 4.4504.10) and by the Swedish Research Council (Contracts No. 2017-00621, No. 621-2014-4501, and No. 621-2015-04990). Computational resources have been provided by the Shared ICT Services Centre of the Université libre de Bruxelles and by the Consortium des Équipements de Calcul Intensif (CÉCI), funded by the Fonds de la Recherche Scientifique – FNRS under Grant No. 2.5020.11. The authors thank the Belgian State for the grant allocated by Royal Decree for research in the domain of controlled thermonuclear fusion. XU is Senior Research Associate of the Fonds de la Recherche Scientifique – FNRS. TL was funded by a fellowship of the Fonds pour la Formation à la Recherche dans l'Industrie et dans l'Agriculture–FRIA.

References

[1] Millar T J, Walsh C, Field T A 2017 *Chem. Rev.* **117** 1765
[2] McCarthy M C, Gottlieb C A, Gupta H and Thaddeus P 2006 *Astrophys. J.* **652** L141
[3] Cernicharo J, Guélin M, Agúndez M, Kawaguchi K, McCarthy M and Thaddeus P 2007 *Astron. Astrophys.* **467** L37
[4] Brünken S, Gupta H, Gottlieb C A, McCarthy M and Thaddeus P 2007 *Astrophys. J.* **664** L43
[5] Thaddeus P, Gottlieb C A, Gupta H, Brünken S, McCarthy M C, Agúndez M, Guélin M and Cernicharo J 2008 *Astrophys. J.* **677** 1132
[6] Cernicharo J, Guélin M, Agúndez M, McCarthy M, and Thaddeus P 2008 *Astrophys. J. Lett.* **688** L83
[7] Agúndez M, Cernicharo J, Guélin M, Kahane C, Roueff E, Klos J, Aoiz F J, Lique F, Marcelino N, Goicoechea J R *et al* 2010 *Astron. Astrophys.* **517** L2
[8] Wakelam V and Herbst E 2008 *Astrophys. J.* **680** 371
[9] Vuitton V, Lavvas P, Yelle R V, Galand M, Wellbrock A, Lewis G R, Coates A J, Wahlund J-E 2009 *Planet. Space Sci.* **57** 1558
[10] Olson R E, Peterson J R, Moseley J 1970 *Geophys. Res.* **76** 2516
[11] Sagawa E, Immel T J, Frey H U and Mende S B 2005 *J. Geophys. Res.* **110** A11302
[12] Qin J, Makela J J, Kamalabadi F Meier R R 2015 *J. Geophys. Res. Space Physics* **120** 10116
[13] Wys, R F G 2016 in *ASP Conf. Ser.* **507** *Multi-Object Spectroscopy in the Next Decade: Big Questions, Large Surveys, and Wide Fields* ed. Skillen I, Balcells M and Trager S (San Francisco, CA: ASP) 13
[14] Asplund M 2005 *Annu. Rev. Astron. Astrophys.* **43** 481
[15] Barklem P S 2016 *Astron. Astrophys. Rev.* **24** 9

[17] Toigo V *et al* 2017 *New J. Phys.* **19** 085004
[18] Fantz U, Franzen P and Wünderlich D 2012 *Chem. Phys.* **398** 7
[19] Bacal M and Wada M 2015 *Appl. Phys. Rev.* **2** *021305*
[20] Le Padellec A, Launoy T, Dochain A and Urbain X 2017 *J. Phys. B: At. Mol. Opt. Phys.* **50** 095202
[21] Staicu-Casagrande E M, Nzeyimana T, Naji E A, de Ruette N, Fabre B, Le Padellec A and Urbain X 2004 *Eur. Phys. J.* D **31** 469
[22] Le Padellec A, Staicu-Casagrande E M, Nzeyimana T, Naji E A and Urbain X 2006 *J. Chem. Phys.* **124** 154304
[23] Phaneuf R A, Havener C C, Dunn G H and Müller A 1999 *Rep. Prog. Phys.* **62** 1143
[24] Nzeyimana T, Naji E A, Urbain X and Le Padellec A 2002 *Eur. Phys. J.* D **19** 315
[25] de Ruette N, Dochain A, Launoy T, Nascimento R F, Kaminska M,Stockett M H, Vaeck N, Schmidt H T, Cederquist H and Urbain X 2018 *Phys. Rev. Lett.* **121** 083401
[26] Chibisov M I and Janev R K 1988 *Phys. Rep.* **166** 1
[27] Zhou X and Dickinson A 1997 *Nucl. Instrum. Methods* B **124** 5
[28] Mitrushchenkov A, Guitou M, Belyaev A K, Yakovleva S A, Spielfiedel A, and Feautrier N 2017 *J. Chem. Phys.* **146** 014304
[29] Belyaev A K 2013 *Phys. Rev. A* **88** 052704
[30] Launoy T, Loreau J, Dochain A, Liévin J, Vaeck N and Urbain X, accepted for publication in *Astrophys. J.* (*Preprint* arXiv:1906.06715)
[31] Thomas R D, Schmidt H T, Andler G, Björkhage M, Blom M, Brännholm L, Bäckström E, Danared H, Das S, Haag N *et al* 2011 *Rev. Sci. Instrum.* **82** 065112
[32] Schmidt H T, Thomas R D, Gatchell M, Rosén S, Reinhed P, Löfgren P, Brännholm L, Blom M, Björkhage M, Bäckström E *et al* 2013 *Rev. Sci. Instrum.* **84** 055115
[33] Schmidt H T, Eklund G, Chartkunchand K C, Anderson E K, Kaminska M, de Ruette N, Thomas R D, Kristiansson M K, Gatchell M, Reinhed P, Rosén S, Simonsson A, Källberg A, Löfgren P, Mannervik S, Zettergren H and Cederquist H 2017 *Phys. Rev. Lett.* **119** 073001